TASK QUARTERLY 5 No 3 (2001), 355–371

DISPERSION OF COLLOIDAL AGGLOMERATE IN MESOSCALE MODELLED BY A HYBRID FLUID PARTICLE MODEL†

WITOLD DZWINEL[1] AND DAVID A. YUEN[2]

[1]*AGH Institute of Computer Science,*
Al. Mickiewicza 30, 30-059 Cracow, Poland
dzwinel@uci.agh.edu.pl

[2]*Minnesota Supercomputer Institute,*
University of Minnesota, Minneapolis,
Minnesota 55415-1227, USA
davey@krissy.msi.umn.edu

(Received 11 June 2001)

Abstract: The dispersion of the agglomerating fluid process involving colloids has been investigated at the mesoscale level by a discrete particle approach – the hybrid fluid particle model (FPM). Dynamical processes occurring in the granulation of colloidal agglomerate in solvents are severely influenced by coupling between the dispersed microstructures and the global flow. On the mesoscale this coupling is further exacerbated by thermal fluctuations, particle-particle interactions between colloidal beds and hydrodynamic interactions between colloidal beds and the solvent. Using the method of FPM, we have tackled the problem of dispersion of a colloidal slab being accelerated in a long box filled with a fluid. Our results show that the average size of the agglomerated fragments decrease with increasing shearing rate Γ, according to the power-law $A \cdot \Gamma^k$, where k is around 2. For larger values of Γ, the mean size of the agglomerate S_{avg} increases slowly with Γ from the collisions between the aggregates and the longitudinal stretching induced by the flow. The proportionality constant A increases exponentially with the scaling factor of the attractive forces acting between the colloidal particles. The value of A shows a rather weak dependence on the solvent viscosity. However, A increases proportionally with the scaling factor of the colloid-solvent dissipative interactions. These results may be applied to enhance our understanding concerning the nonlinear complex interaction occurring in mesoscopic flows such as blood flow in small vessels.

Keywords: fluid particle model, mesoscopic flow, colloidal agglomerate, fragmentation, agglomeration

1. Introduction

Mesocopic flows are important to understand because they hold the key to the interaction between the macroscopic flow and the microstructures. This is especially true in colloidal flows, which involve colloidal mixtures, thermal fluctuations and particle-particle interactions. In many technological and physical processes, such as emulsification, formation

† Extended version of this lecture is submitted to *J. of Colloids and Interface Sci.*

of nanojets [1], water desalination, food production, gel filtration and transport processes in magma melts or in tiny blood vessels, the microscopic or microstructural effects may even dominate over the hydrodynamical processes and these phenomena take place in the realm of mesoscopic flows.

There exists a large body of knowledge on the theoretical, experimental and numerical models dealing with various aspects of flow of powdered solids in liquid [2]. However, colloidal beds cannot be treated as a dry powder. In general sense, colloids comprise two types of particles – large and small ions, which are suspended in a solvent. Colloidal agglomerates consist of large ions due to complex ion-ion and ion-solvent interactions, which are of entropic and electrostatic origin [3]. The classical models of powder granulation in liquids assume that the Péclet number is much greater than unity and the agglomerate size is much larger than the interaction range of cohesion forces [2]. This means that thermal fluctuations, diffusion effects in liquid and microscopic interactions are neglected. For these assumptions the fragmentation microstructurs such as rupture, erosion, shatter, and aggregation process can be considered separately. In the mesoscale, with the presence of diffusion, thermal fluctuations and long-range interactions between colloidal particles, fragmentation and aggregation microstructures usually occur simultaneously or overlap.

Since blood can be regarded as a colloid [4], we will use this as an example for explaining the rationale of our modelling. The axisymmetric pulsatile flows and flows subject to acceleration in blood vessels have been investigated both experimentally and numerically for a long time (see *e.g.* [5–8]). These investigations were focused on the influence of material damping on the wall vessels, the viscoelastic properties [9] of blood on the flow, deformation properties of blood vessels from the shear stresses exerted on the wall and the mass transfer and fluid dynamics of blood flow. All of these phenomena can be simulated by using Navier-Stokes equations with proper substitution of the blood rheological properties. However, there are many medical circumstances in which the Navier-Stokes equations with simple rheology may not work and they are rapid heart-attack or a rapid stroke developed by sudden clotting in small blood vessels. These are critical phenomena in which a transition has taken place in the microscale and propagate over to the mesoscale. In this mesoscale regime, the blood's rheology has changed and should be treated as a complex fluid with various kinds of microstructures, which have suddenly been developed. A review of the relevant concepts in block of microcirculation in blood vessels was first given by [10]. Until now there has not been much progress made in the field in these aspects concerning the flow interactions between the microstructural dynamics and the larger-scale flow. The modelling of the dispersion of drugs and thrombus along tiny blood vessels needs a completely different approach, which is still in the air. In this paper we will model the colloidal interactions between these recently formed microstructures with the complex types of flows by means of a discrete particle model.

Microscopic techniques employing discrete particles such as molecular dynamics (MD) and Monte Carlo (MC) are very useful in studying interactions between primary particles, which form molecules and microstructures. For example, the large-scale MD simulations were employed for investigating microscopic flows [11, 12, 1] and microstructures in solid materials such as impurities in crystals and cracks [13]. However, MD becomes too demanding for simulating larger particle ensembles. At the present time the particle systems of size about one micrometer during tens of nanoseconds can be simulated by using

10^9 atoms on the largest parallel computers [13]. Most of the computations spend time on producing information on microscopic fluctuations, which is not necessary for scales in the ordering of complex fluids.

In recent years, beside classical models, new numerical methods have been developed for modeling physical and chemical phenomena occurring in the mesoscale. The most popular are: lattice Boltzmann gas (LBG) [14–16], diffusion limited aggregation [17], direct numerical simulations (DNS) [18, 19] or other particle methods such as stochastic rotational dynamics (SRD) [20], fluid particle dynamics (FPD) [21], dissipative particle dynamics (DPD) [22] and fluid particle model (FPM) [23].

Dissipative particle dynamics (DPD) is one of the mesoscopic techniques, which allows one to model hydrodynamic behavior with thermal fluctuations. This particle based off-lattice algorithm was inspired by the ideas coupling the advantages of both the molecular dynamics and lattice-gas methods. A strong background drawn from statistical mechanics has been provided to DPD [24], from which explicit formulas for transport coefficients in terms of the particle interactions can be derived. Since then the DPD model has attracted a great deal of attention from the chemical community.

As shown in [25, 26], DPD can be used for studying various types of phase separation processes in binary or multicomponent fluids. By employing two-level model for which colloidal beds are modeled by MD particles and solvent by DPD fluid particles, one can simulate miscellar solutions [27] and large colloidal aggregates, which can use as many as 20 million particles [28]. Dissipative particle dynamics can also be employed for simulating hydrodynamical instabilities such as thin-film falling down the inclined plane [29], the breakup of droplets and mixing in complex fluids [30–32].

For simulating mixing of colloidal agglomerates, over the mesoscale, we have implemented generalized version of dissipative particle dynamics DPD devised by Español [23] together with the fluid particle model (FPM), which is hybridized within the framework of a classical MD code. We will first describe the model. We then present the results from the FPM simulations. Finally we summarize our findings and discuss the prospects of employing the discrete particle method for modelling dynamics of complex colloidal fluid in the mesoscale.

2. Description of the fluid particle model (FPM)

We begin our discussion by first going over some rudiments of the dissipative particle dynamics (DPD) method [22]. The DPD technique portrays the mesoscopic portions of a real fluid. They can be viewed as "droplets" of liquid molecules with an internal structure and with some internal degrees of freedom. As shown in [24, 23], the interactions between these particles are postulated from simplicity and symmetry principles. These principles ensure their correct hydrodynamic behavior. The advantage of DPD over other methods, such as lattice-gas or lattice-Boltzmann, lies in the possibilities of matching the scale of discrete-particle simulation to the dominant spatio-temporal scales of the entire system [23].

One of the serious drawbacks of DPD is the absence of a drag force between the central particle and the second one orbiting about the first particle. This relative motion may produce a net drag, when many DPD particles are participating at the same time [23]. This cumulative effect would reduce the computational efficiency of the DPD method. For this reason, the fluid particle method (FPM) has been introduced by means of a non-central force,

which is proportional to the difference between the velocities of the particles [23]. This will eliminate this deleterious effect from the net drag force. Additionally, this FPM approach would allow for the simulation of physical effects associated with rotational diffusion and rotation of the colloidal beds resulting from hydrodynamic or their mutual interactions.

The theoretical framework for the FPM was presented by Español [23]. We retain here the original notation used in [23]. The fluid particles posses several attributes as mass m_i, position r_i, translational and angular velocities and type. The "droplets" interact with each other by forces dependent on the type of particles. We use the two-body, short-ranged force $\mathbf{F}$ as it is postulated in [23]. This type of interaction is a sum of conservative $\mathbf{F}^C$, two dissipative components $\mathbf{F}^T$ and $\mathbf{F}^R$ and a Brownian force $\tilde{\mathbf{F}}$, that is:

$$\mathbf{F}_{ij} = \mathbf{F}^C_{ij} + \mathbf{F}^T_{ij} + \mathbf{F}^R_{ij} + \tilde{\mathbf{F}}_{ij}. \tag{1}$$

The FPM force components are defined by:

$$\mathbf{F}^C_{ij} = -V\left(r_{ij}\right)\cdot\mathbf{e}_{ij}, \tag{2}$$

$$\mathbf{F}^T_{ij} = -\gamma\cdot m\mathbf{T}_{ij}\cdot\mathbf{v}_{ij}, \tag{3}$$

$$\mathbf{F}^R_{ij} = -\gamma\cdot m\mathbf{T}_{ij}\cdot\left(\frac{1}{2}\mathbf{r}_{ij}\times\left(\boldsymbol{\omega}_i+\boldsymbol{\omega}_j\right)\right), \tag{4}$$

$$\tilde{\mathbf{F}}_{ij}dt = (2k_BT\gamma\cdot m)^{1/2}\left(\tilde{A}\left(r_{ij}\right)d\bar{\mathbf{W}}^S_{ij} + \tilde{B}\left(r_{ij}\right)\frac{1}{D}tr\left[d\mathbf{W}\right]1 + \tilde{C}\left(r_{ij}\right)d\bar{\mathbf{W}}^A_{ij}\right)\cdot\mathbf{e}_{ij}, \tag{5}$$

where:

r_{ij} – is a distance between particles i and j, $\mathbf{r}_{ij} = \mathbf{r}_i - \mathbf{r}_j$ is a vector pointing from particle i to particle j and $\mathbf{e}_{ij} = \mathbf{r}_{ij}/r_{ij}$,

D – is the dimensionality of the model,

T – is the temperature of particle system,

k_B – the Boltzmann constant,

dt – is the timestep,

γ – scaling factor for dissipation forces,

$\boldsymbol{\omega}$ – angular velocity,

$d\mathbf{W}^S$, $d\mathbf{W}^A$, $tr[d\mathbf{W}]\mathbf{1}$ – are symmetric, antisymmeric and trace diagonal random matrices of independent Wiener increments defined in [23],

$A(r)$, $B(r)$, $C(r)$, $\tilde{A}(r)$, $\tilde{B}(r)$, $\tilde{C}(r)$, $V'(r)$ – functions dependent on the separation distance $r = r_{ij}$.

$\mathbf{T}_{ij}$ is a dimensionless matrix given by:

$$\mathbf{T}_{ij} = A\left(r_{ij}\right)\mathbf{1} + B\left(r_{ij}\right)\mathbf{e}_{ij}\mathbf{e}_{ij}, \tag{6}$$

$\mathbf{1}$ – is the unit matrix.

As was shown in [23] the single component FPM system yields the Gibbs distribution as the steady-state solution to the Fokker-Planck equation under the condition of detailed balance. Consequently it obeys the fluctuation-dissipation theorem, which defines the relationship between the normalized weight functions, which are chosen such that:

$$A(r) = \frac{1}{2}\left[\tilde{A}^2(r) + \tilde{C}^2(r)\right], \quad B(r) = \frac{1}{D}\left[\tilde{B}^2(r) - \tilde{A}^2(r)\right] + \frac{1}{2}\left[\tilde{A}^2(r) - \tilde{C}^2(r)\right]. \tag{7}$$

For the dissipative particle dynamics (DPD) method $A(r) = 0$, consequently $\tilde{A}(r)$, $\tilde{B}(r)$, $\tilde{C}(r) = 0$ and $V'(r) \propto B(r)$, which means that all the DPD forces are central.

The non-central force in FPM, which is proportional to the difference between particle velocities, introduces an additional drag lacking in the DPD model. The non-central force results also in additional rotational friction given by Equation (4).

The temporal evolution of the particle ensemble obeys the Newtonian laws of motion:

$$\dot{\mathbf{v}}_i = \frac{1}{m}\sum_{i\neq j}\mathbf{F}_{ij}, \tag{8}$$

$$\dot{\mathbf{r}}_i = \mathbf{v}_i, \tag{9}$$

$$\dot{\boldsymbol{\omega}} = \frac{1}{I}\sum_{i\neq j}\mathbf{N}_{ij}, \tag{10}$$

where the torques are given by:

$$\mathbf{N}_{ij} = -\frac{1}{2}\mathbf{r}_{ij}\times\mathbf{F}_{ij}. \tag{11}$$

The FPM method can predict precisely the transport properties of the fluid, thus allowing one to adjust the model parameters according to the formulas of kinetic theory. Unlike in macroscopic particle based method – smoothed particle dynamics SPH [33] – the angular momentum is conserved exactly in FPM. In short, the FPM model can be physically interpreted as a Lagrangian discretization of the non-linear fluctuating hydrodynamic equations.

3. Numerical model

We have employed a two-dimensional model of a simulation involving clearly a three-dimensional process. However, the simplified 2-D models are less time-consuming than 3-D models and we can certainly glean some useful basic information before venturing into the 3-D arena. It is a matter of more computer time to carry out 3-D simulations in FPM.

This is a two-level approach and we will consider two types of particles: solvent droplets and colloidal beds. We assume that the concentration of electrolyte in the solvent is low, which is appropriate for the blood. In this case we can neglect the long-range interactions and focus just on the short-range forces. Therefore, the electrolyte-solvent particles can be represented by FPM fluid particles.

We assume that the weight functions (Equations (6) and (7)) satisfy the conditions imposed. Due to degree of a freedom allowed by the model in selecting the weight functions we may assume that:

$$\tilde{A}(r) = 0, \quad A(r) = B(r) = \left(1 - \frac{r}{r_{cut}}\right)^2, \quad V'(r) = -\Pi\cdot\frac{3}{\pi\cdot r_{cut}^2 n}\left(1 - \frac{r}{r_{cut}}\right), \tag{12}$$

where, r_{cut} – is a cut-off radius, which defines the range of particle-particle interactions. For $r_{ij} > r_{cut}$, $\mathbf{F}_{ij} = 0$.

The first assumption is recommended in [23]. We postulate the rest of weight functions the same as in DPD [22, 24]. Due to additional drag between particles caused by the non-central interactions we can reduce the computational load assuming that the interaction range is shorter than for DPD fluid.

The colloidal agglomerates consist of primary particles – the colloidal beds. They can represent large charged ions, which are a few times larger than electrolyte-solvent droplets. We assume that the agglomerates are "wet", *i.e.*, colloidal beds are covered by electrolyte

binder. This assumption allows us to use in the model mean forces similar to those obtained for charged macro ions in realistic colloidal mixtures.

Interactions among colloidal particles have been studied for more than 50 years. Colloids can be regarded as complex many-body systems described by highly approximate treatments drawn from classical statistical physics. As follows from the conventional (Derjaguin, Landau, Verwey, Overbeek) DLVO theory the long-range electrostatic interaction between colloidal spheres can be modelled by a screened-Coulomb repulsion [34]. Additional interactions come from hydrodynamic [35] and depletion forces [36]. Some experimental findings [37, 35] show that like-charged macro ions have been attracted to one another by short ranged forces. This fact cannot be explained by the conventional theories. The recent simulation results [3] show that the fluctuation of the charge distribution by the small ions results in the attraction between micro ions. The mean force is a combination of hard-sphere and electrostatic force. As an approximation $V(r_{ij})$ (see Equation (2)) of the mean force between colloidal beds, we use the sum of the Lennard-Jones (L-J) force and a very steep force with a soft core. In Figure 1 we depict that the approximation is very close to the mean force obtained from large-scale Monte-Carlo calculations performed for a real colloidal mixture [3]. The force well is proportional to ε – the minimum of L-J potential – which is called here the cohesion factor. Unlike in our previous papers exploiting two-level model [27, 28, 31], we introduce additional non-central dissipative force between colloidal beds. This force is responsible for dissipation of energy due to bed collisions. The colloidal particles are larger and heavier than FPM "droplets" and their interactions are singular. Therefore, thermal fluctuations are transferred from the bulk of fluid and are partly dissipated inside the colloidal agglomerates ($\tilde{\mathbf{F}} = 0$, if i and j are colloidal particles). There is also no drag between colloidal beds ($B(r_{ij}) = 0$) because the binder layer covering colloidal beds is assumed to be very thin.

The bed-"droplet" interactions are simulated by employing FPM forces. This is justifiable on the following grounds:

- the bed-"droplet" forces cannot be singular,
- non-zero Brownian component ($\tilde{\mathbf{F}}_{ij} \neq 0$) comes from the fluid "droplet",
- viscous drag ($B(r_{ij}) \neq 0$) comes from the fluid "droplet" and the electrolyte binder,
- the electrolyte concentration in electrolyte-solvent mixture surrounding the agglomerate is low, thus electrostatic bed-"droplet" interactions are negligibly small.

Because the colloidal bed contains a hard core, we have modified repulsive part of conservative $\mathbf{F}^C$ bed-"droplet" forces, thus making it steeper than for "droplet"-"droplet" interactions.

The FPM model is based on concepts drawn from statistical physics. In contrast to DPD and two-level models used in our earlier simulations, it is a more general and self-consistent particle method. Simulation of multiphase flow consists in appropriate definition of conservative forces between particles representing different phases and in setting some interactions to zero. Thermodynamic properties of the model and the detailed balance conditions are always preserved according to the rigorous theoretical basis set out in [23, 38].

The forces are computed by using $O(M)$ order (M-number of particles) link-list scheme combined with neighbor tables [39]. Multiple link-lists are used because the sizes

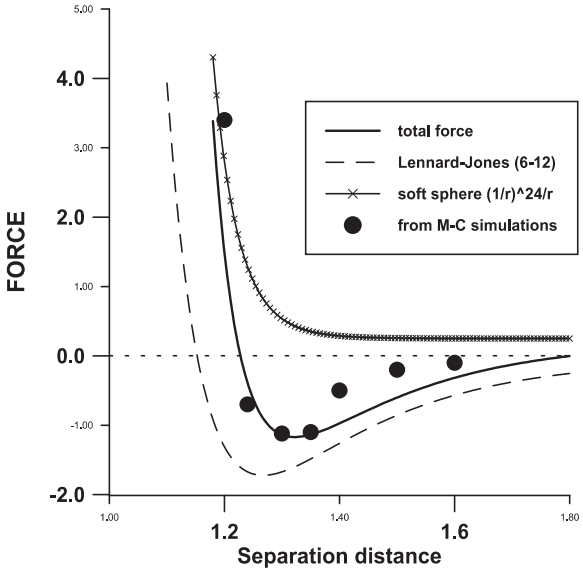

Figure 1. The mean force between colloidal particles as a function of macro ion separation (in units of macroion diameter) approximated by the sum of the L-J force and soft sphere repulsion. Black dots show the approximate shape of the mean force obtained from Monte-Carlo simulation of a macro ions interactions in a real colloidal mixture [3]

of particles and ranges of interactions ($\mathbf{r}_{cut}$) are different, that is, larger Hockney cells [39] are used for longer ranged interactions.

In the integration of the equations of motion, we have employed the *leap-frog* numerical scheme. Due to large instabilities observed by using *leap-frog* for angular velocity computations, we have used the following higher-order temporal $O(\Delta t^4)$ scheme for ω:

$$\boldsymbol{\omega}_i^{n+1/2} = 2\boldsymbol{\omega}_i^{n-1/2} - \boldsymbol{\omega}_i^{n-2/3} + \left(\mathbf{N}_i^n - \mathbf{N}_i^{n-1}\right). \tag{13}$$

The values of $\mathbf{v}^{n+1}$ and $\boldsymbol{\omega}^{n+1}$ are predicted by using $O(\Delta t^2)$ Adams-Bashforth procedure as it is in [26].

The parameters associated with the fluid dynamical interactions of FPM have been matched to the fluid transport coefficients by using the equations in the continuum limit and the detailed balance condition [39]:

$$P_{k\neq l} = \frac{n \cdot \Pi_{k\neq l} \langle r \rangle}{2 \cdot D}, \tag{14}$$

$$\nu_b = \gamma \cdot n \left[\frac{A_2}{2D} + \frac{D+2}{2D} B_2 \right] + c^2 \frac{1}{\gamma \cdot Dn\,(A_0 + B_0)}, \tag{15}$$

$$\begin{aligned} A_0 &= \frac{1}{D} \int d\mathbf{r} A(r), \quad B_0 = \frac{1}{D(D+2)} \int d\mathbf{r} B(r), \\ A_2 &= \frac{1}{D} \int d\mathbf{r} r^2 A(r), \quad B_2 = \frac{1}{D(D+2)} \int d\mathbf{r} r^2 B(r), \end{aligned} \tag{16}$$

$$\gamma = \frac{\sigma^2 m}{2 k_B T}, \tag{17}$$

where P – is a partial pressure, T_0 – temperature of the particle system, ν_b – is a bulk kinematic viscosity, $D = 2$, $c^2 = k_B T/m$, Π, σ and γ – scaling factors of conservative, Brownian and dissipative forces, respectively.

The results of our test runs show that our FPM model satisfy the basic physical constraints:

- Total angular and translational momenta are preserved,
- The actual thermodynamical pressure computed from the virial theorem is constant. Its average is $5-10\%$ larger than P assumed (for $M = 50\,000$ particles),
- The actual thermodynamical temperature computed from the average kinetic energy of the particle system is constant and deviates no more than 2–5% from the value of T,
- The rotational kinetic energy is about 1/3 of the total kinetic energy.

Since the compressibility of the fluid is low (for a large value of Π), there are some quantitative differences between the theory and the simulation. The kinetic theory formulas have been developed in the limit where no conservative forces are present. The actual transport coefficients computed from generalized Einstein and Green-Kubo formulas [40] are larger more than 50% than those predicted from the classical kinetic theory [41]. Therefore, the transport coefficients computed from the theory can be used only as the first coarse approximation. The most precise matching can be done by using a new generic formulation of DPD model, which is a natural generalization of both the DPD and FPM [38].

Table 1. Program units

Value	Unit
Length λ	the average distance between the neighboring fluid particles
Mass m	dimensionless – mass of the lightest fluid particle $m = 1$
Time t	in $t = \lambda/c$ where $c^2 = k_B T/m$, λ – unit of length
Energy ε	in $\frac{3}{2}k_B T$ (average kinetic energy for Maxwell distribution)
Viscosity Ω	$\Omega = \gamma r_c/2 \cdot c$ where γ is the scaling factor of dissipative forces

We have solved the problem for finding clusters of very sophisticated shapes created during granulation by employing an efficient $O(M)$ clustering procedure. It is based on the mutual nearest neighboring (mnn) distance concept. This procedure is outlined in [28].

To define the transport properties of liquid, we introduce dimensionless factor Ω as it is in [42]:

$$\Omega = \gamma r_c / D \cdot c, \tag{18}$$

where D is dimension of the system. The value of Ω represents the magnitude of the viscous FPM forces. We introduce also the other dimensionless units collected in Table 1.

Table 2 comprises the principal dimensionless parameters used in 2D simulations. We assume that:

- density of colloidal system is 10 times greater than density of the liquid,
- spacing between colloidal beds is 50% greater than for liquid "droplets".

Since the droplets represent clusters of molecules, we can estimate that a colloidal bed is around a few orders of magnitude larger than a molecule, which would put it around 0.1 to 1 micron.

The existence of the non-central force in the FPM, allows us employing a shorter cut-off radius for forces calculation than in DPD simulations thus saving computational time. A typical cut-off radius used in DPD simulation is 2.5λ [22, 25]. The number density

Table 2. Principal physical and numerical parameters

General parameters	Values		
T [K]	50		
g	$0.00001\ \lambda/\Delta t^2$		
Δt	0.008		
	Types of interactions		
	Liquid particle–Liquid particle	Liquid particle–Colloidal bed	Colloidal bed–Colloidal bed
Average distance between neighboring particles λ	1	1.5	1.5
Number density	3.2 (particles in sphere of radius λ)	3.2	3.2
Cut-off radius (in λ)	1.5	2.5	1.8
Particle mass	$m_1 = 1$	$m_{1,2} = \frac{2m_1 m_2}{m_1 + m_2}$	$m_2 = 22.5$
Sound velocity $\sqrt{\frac{P}{\rho}}$ (in c)	7.4	—	1.5
Viscosity	25	25	10
Cohesion factor ε	—	—	0–4
Number of particles (for large-scale $R-T$ simulations)	1×10^5 (1×10^6)	— —	2×10^3 (5×10^4)

from Table 2 is also representative for MD and DPD simulations of liquids in 2D. The partial pressure P is relatively high, thus resulting in a very incompressible liquid.

We consider a colloidal slab accelerated in a periodic box. Similar types of flows were studied for solid-liquid mixing by assuming a constant shear rate [2]. By using an accelerated flow we can investigate the granulation of colloidal agglomerate over a broad range of kinetic energies in the flow with a single simulation. The particles are confined within the rectangular box with periodic boundary conditions in y-direction and reflecting walls in x-direction. The aspect ratios of the slab to the box dimensions are 1 : 5 and 1 : 10 along x and y axes, respectively. As shown in Figure 2, the V-shaped profile of velocity field stabilizes after about 15 000 timesteps. Over the whole periodic box along both the x and y directions we can observe strong correlations along the horizontal direction. The vertical correlations are weaker due to greater aspect ratio and vanishing velocity gradients in y direction. In the following section we report the simulation results of granulation for this type of flow.

4. Dispersion of colloidal slab in a periodic box

In Figures 3 and 4 we present the snapshots from 2-D FPM simulations of dispersion of colloidal agglomerate accelerated in a periodic box.

We recognize several tages of granulation, which usually occur with some degree of overlap:

1. **Imbibition** – consisting in spreading off the liquid solvent into the colloidal cluster, and reducing the cohesive forces between the colloidal beds. This process corresponds to the wetting of a dry, porous solid by the liquid.

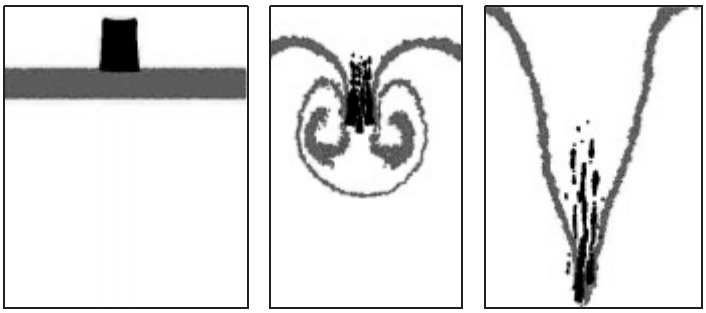

Figure 2. Velocity profiles with simulation time. The V-shaped profile becomes stable after about 15 000 timesteps

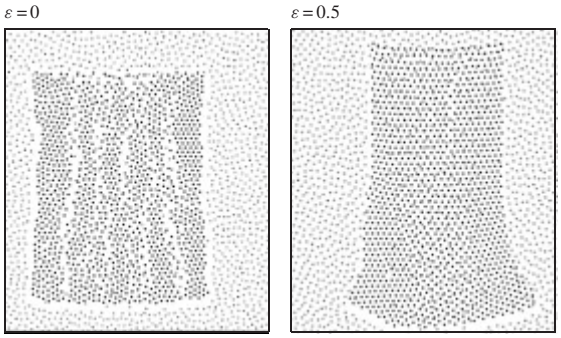

Figure 3. Imbibition of colloidal agglomerate by fluid particles for different cohesion factor ε; $T = 3\,000$

2. **Fragmentation** – consisting of **shatter** – producing a large number of smaller fragments in a single event, **rupture** – breakage of a cluster into several fragments of comparable size, **erosion** – gradual shearing off of small fragments of comparable size [2],
3. **Aggregation** – the process being the reverse of dispersion. Two traditional mechanisms can be recognized: **nucleation** – defined as the gluing together of primary particles due to the attractive forces, **coalescence** – is the process by which two larger agglomerates combine to form a granule.

Imbibition is the principal mechanism responsible for initiating fragmentation. As shown in Figure 3, fluid particles penetrate the permeable agglomerate. The repulsive forces between colloidal and fluid particles (see Equation (12)) reduce the attractive interactions between colloidal beds. In the case where there is a lack of cohesive forces between the primary particles and $\varepsilon = 0$, the fluid particles create longitudinal paths parallel to the streamlines (see Figure 3). Simulation results from Figure 4 ($\varepsilon = 0$) show that for longer simulation times ($T = 5\,000 - 7\,500$) the slab brakes up (shatter) along these paths. For larger value of ε (see Figures 3 and 4), fluid particles concentrate in the center of agglomerate. Unlike the case without any cohesive forces ($\varepsilon = 0$), the presence of cohesive force allows one to observe the crosswise fragmentation of the colloidal slab.

Fragmentation may be caused by a few mechanisms. Rupture or shatter of the slab from Figure 4 for $T = 5\,000 - 7\,500$ is the consequence of cracks formed at the initial stages

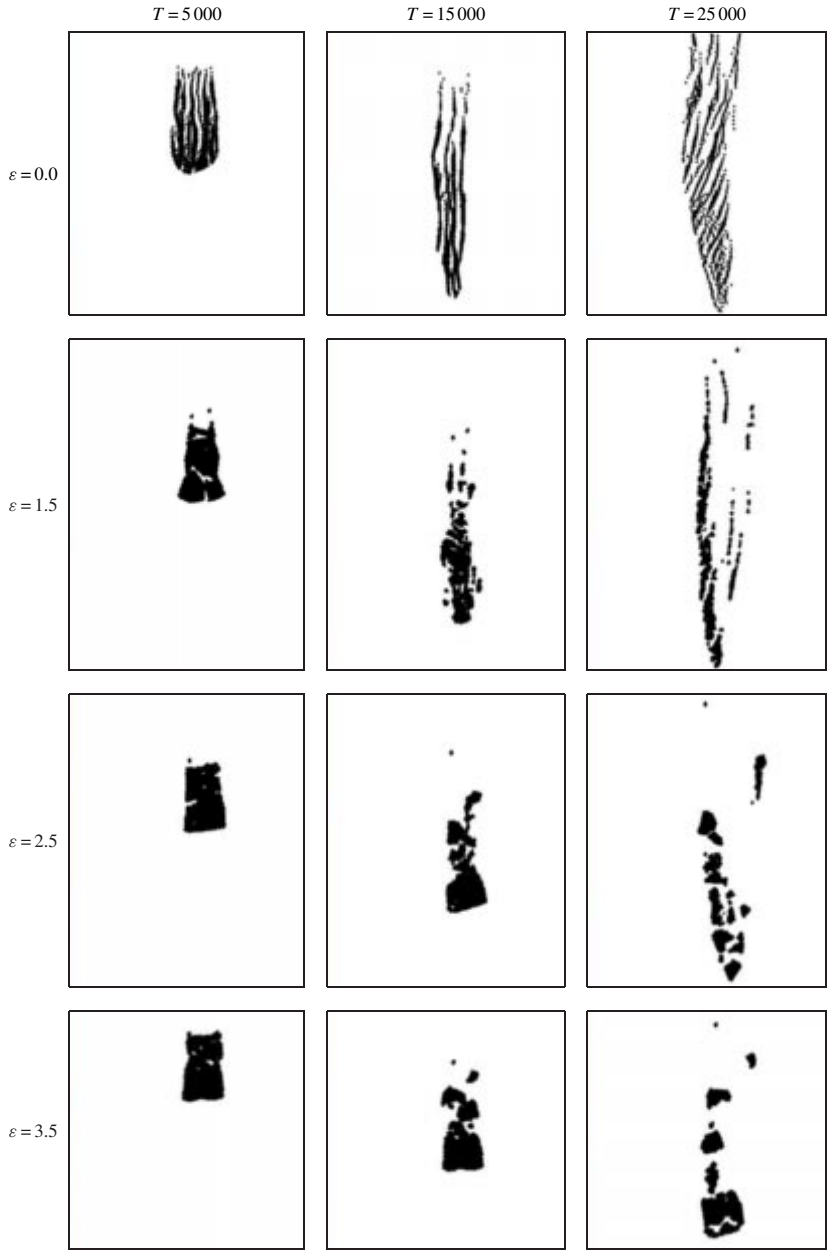

Figure 4. Selected snapshots from FPM simulations of accelerated colloidal slab in a periodic box for various cohesion factors ε

of simulation. The formation of cracks is due to direct compressive loads and particle-particle impacts than to the hydrodynamical forces. The relevance of hydrodynamic forces in fragmentation shows up at greater kinetic energies of the flow.

The dimensionless number, which characterizes fragmentation, the fragmentation number Fa is defined as follows:

$$Fa = \frac{\mu\Gamma}{\mathbf{T}}, \tag{19}$$

where:
μ – dynamic viscosity,
T – denotes the cohesive strength,
Γ – shearing rate:

$$\Gamma = V/\delta s, \tag{20}$$

V – a characteristic velocity,
δs – a characteristic length scale for the Stokes flow.

The agglomerate strength **T** is not an intrinsic material property, like the surface tension but depends on many factors, including the internal structure, compaction and many other physical parameters.

When the fluid dynamical stresses exceed a critical value Fa_{crit}, that is, $Fa > Fa_{crit}$, the agglomerates would rupture in the shear flow. As shown in [2], for fragmenting polystyrene lattices the value of Fa_{crit} is reciprocal of the mean agglomerate size S_{avg}. Ionic effects at high electrolyte concentrations are well accounted for by assuming **T** to be proportional to the force between two primary particles, *i.e.*, $\mathbf{T} \approx g(\varepsilon)$ where ε is here a maximum cohesion strength – the cohesion factor.

Thus the value of **T** is independent on the agglomerate size and the shear rate. From Equations (19)-(20) we obtain:

$$S_{avg} \approx \frac{g(\varepsilon)}{\mu\Gamma}, \tag{21}$$

where $g(\varepsilon)$ is a monotonically increasing function of ε determined empirically [2]. A similar relationship between the mean cluster size and the shear rate Γ is also found in the case of converging flow and in the granulation of wet agglomerate in powder due to the shear flow.

Mixing and segregation of granular materials can be simulated also employing discrete particle model rooted in molecular dynamics simulations. The rapid granular flow simulation (RGFS) employs actual expressions for the magnitude of the forces for describing the interactions between the finite-sized particles [21]. Interactions between particles in RGFS are restricted to frictional effects and elastic and plastic deformations of the surface, which limits the applicability of these models to dry powder flows. The agglomeration of fine particles in wet granulation can be achieved by introducing an intermediary viscous binder fluid into a shearing mass of powder [21]. Viscous interactions between solid particles covered by the binder allow the particles to adhere together or bounce off one another. The wet agglomerates breakup in a shear flow. The wet agglomerates rupture when the Stokes number St – determined by the ratio of the initial kinetic energy in the shearing mass and the energy resisting deformation – exceeds a critical value.

According to [21], the stable cluster size at the point of equilibrium before deformation and breakup is given by the following formula:

$$S_{avg} \approx \left(\frac{\mu}{\Gamma}\right)^{\alpha}, \tag{22}$$

where μ – dynamic viscosity of fluid binder and $\alpha = 1$ for $\mathbf{T} = \text{const}$. Since cohesive strength **T** will depend on shear rate and/or the size of granule, the value of α is greater than 1. The results from RGFS simulations show that, for a small capillary number (Ca) the value of $\alpha = 2$ (for $Ca > 10$, $\alpha = 5$).

In the both cases, *i.e.*, powder-in-liquid and mud-in-powder flows, the microscopic effects such as the thermal fluctuations can be neglected and shear rate is constant. In the

FPM model, thermal fluctuations in the solvent are simulated by the Brownian component of particle-particle forces. The fluctuations are transferred to the agglomerate particles.

The shear rate Γ changes in time and is defined as follows:

$$\Gamma = \frac{\sqrt{\mathbf{v}_{dif} \cdot \mathbf{v}_{dif}}}{\lambda} \quad \text{where} \quad \mathbf{v}_{dif} = \langle \mathbf{U}_{bed} \rangle - \left\langle \mathbf{U}_{fluid} \right\rangle, \tag{23}$$

where λ is the average distance between the neighboring beds, $\langle \mathbf{U}_{bed} \rangle$ and $\left\langle \mathbf{U}_{fluid} \right\rangle$ are the average translational velocities in y-direction for the agglomerate beds and fluid particles, respectively.

From Figure 5a one can discern that in the beginning the average kinetic energy E_K of the accelerated slab increases with time linearly. After incipient rupture, the value of E_K decreases (compare **Nclu** time dependence from Figure 5b with the plot from Figure 5a). This drop in kinetic energy is due to larger dissipation caused by an increase of friction surface and increase of potential energy of the colloidal particle system after rupture. As shown in Figure 5a, the second mechanism dominates at stronger cohesion. In the course of the simulation, the V-shaped velocity field (Figure 2) causes the colloidal beds concentrate in the center of the box where the velocity is the highest. This mechanism dominates over the previous two after 10 000–13 000 timesteps. The kinetic energy of the colloidal beds increases. Together with an increase of kinetic energy, the agglomerate deforms by creating elongated structures, which then rupture and are eroded.

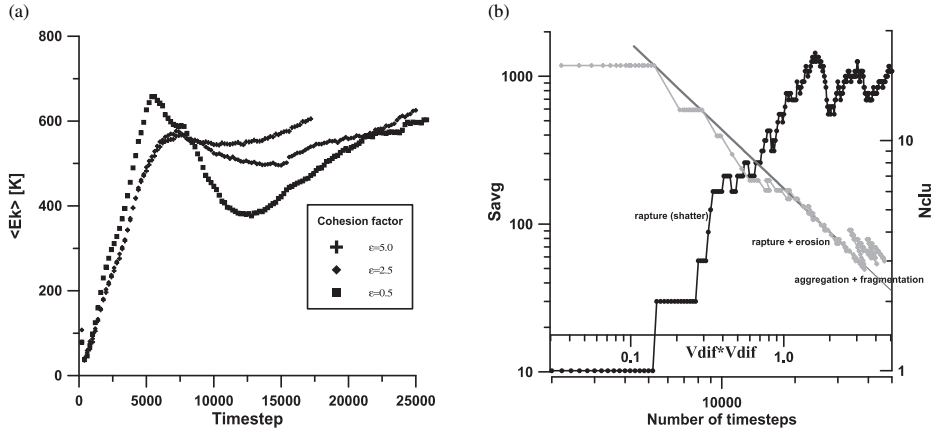

Figure 5. (a) The average kinetic energy of the colloidal agglomerate with time for various cohesion factors ε. (b) Mean cluster size (S_{avg} – gray) with shear rate Γ and number of clusters (N_{clu} – black) with number of timesteps for the colloidal slab accelerated in a periodic box. The value of $\varepsilon = 1.5$. The scales of shear rate Γ and number of timesteps do not correlate exactly

As shown in Figures 5b and 6, in this power-law regime the mean cluster size is as follows:

$$S_{avg} = \frac{A(\varepsilon, \Omega, T_0, \ldots)}{\Gamma^{\alpha}}, \tag{24}$$

where $\alpha \approx 2$ and $A()$ is a function of material properties and physical conditions of the particle system such as temperature, viscosity, partial pressure. The value of α obtained from a linear regression for the different simulation parameters is found to locate within the [1.82,2.12] interval.

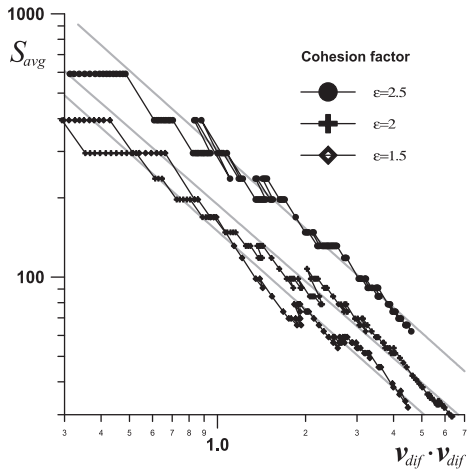

Figure 6. Mean cluster size with time for a few different cohesion factors

This result is, surprisingly, similar to that obtained from RGFS (rapid granular flow simulations) simulations [21] of mud-in-powder shearing flow. The value of α is greater than 1 (as it is in Equation (21)) because the cohesive strength depends on the shear rate and the size of granule. For an increasing shear rate, the temperature of a colloidal granule increases because the energy from friction cannot be dissipated away. Thus there is a positive feedback, since the cohesive strength decreases sharply.

5. Concluding remarks

In this work we have presented results taken from 2-D fluid particle modelling in which we have simulated the flow of a colloidal slab along a long periodic box.

The first type of flow may be applied to blood flow. In both types of solid-liquid flows we can easily recognize the characteristic dispersion caused by the microstructural dynamics and they include phenomena such as rupture, erosion, shatter and agglomeration, all of which would be very difficult to be modelled with conventional continuum methods. We have studied rather thoroughly the process of fragmentation in the power-law regime [2]. In solid-liquid systems, such as the fractal agglomerate in solvent and wet granulation in powder under shear, the mean cluster size S_{avg} varies with the shear-rate Γ as $1/\Gamma^{\alpha}$. This very important relationship can also be detected in mesoscopic solid-liquid systems in which thermal fluctuations play a definite role. In Table 3 we categorize the various types of fragmentation with the mean cluster size.

Table 3. Types of fragmentation with the mean cluster size

Mean cluster size – S_{avg}	Type of fragmentation
$S_{avg} \approx \dfrac{g(\varepsilon)}{\mu\Gamma}$	fractal agglomerate in fluid (experimental)
$S_{avg} \approx \left(\dfrac{\mu}{\Gamma}\right)^2$	wet agglomerate in powder (simulation)
$S_{avg} = \dfrac{b_5 \cdot f(\Omega_{1-1}) \cdot e^{b_4 \cdot \varepsilon}}{\Omega_{1-2}\Gamma^2}$	dense agglomerate accelerated in mesoscopic liquid (simulation)

1. For wet granulation in powder and mesoscopic solid-liquid fragmentation the mean agglomerate size depends inversely on the square of the shear rate. For both cases the cohesive strength **T** depends on shear rate and/or the size of a granule.

2. For shear flow with a constant rate and a constant cohesive strength **T** in fractal agglomerate-in-liquid, the average mean size of the granule varies as $1/\Gamma$.

3. The attractive forces arising from the binder fluid covering the colloidal beds are found to correspond to the dissipative forces in the mesoscopic colloidal agglomerate.

4. The hydrodynamic forces developed in fractal-agglomerate/liquid system would correspond to the dissipative colloidal-bed/fluid-particle interactions in the mesoscale.

5. The exponential dependence of S_{avg} on the cohesive factor epsilon is derived from collective mesoscopic effects, such as short-ranged, attractive ion-ion forces and thermal fluctuations.

Another aspect concerning complexity is revealed by the strong heterogeneity in the flow structure. With the fluid-particle model one can discern properly the multiscale character of the solid-fluid system. These multiscale structures are complicated due to the inflexibility of the description level with varying scale of observation. Unlike [43], where different numerical methods were employed for describing the particle, cluster and the entire system, the FPM model is sole numerical paradigm in our simulations. From a computational standpoint, we do not observe any methodological disparity of solid-fluid interaction mechanisms in totally different regimes in which either fluids or particles may dominate.

Even though the fluid particle model is superior to the older mesoscopic scheme – dissipative particle dynamics – it does not solve the serious conceptual problem of the method of DPD. The thermodynamic behavior of the fluid particle model is determined by the conservative forces, which are soft in comparison with the singular MD interactions. Hence, there does not exist a well-defined procedure to relate the shape and amplitude of the conservative forces with a prescribed thermodynamic behavior. Furthermore, it is not clear what are the physical time and length scales the model actually describes. The presence of thermal noise suggests a fuzzy area belonging to the mesoscopic realm. In [26–28] we show, for example, that the DPD and FPM fluid structures resemble short chain polymers. Serrano and Español [38] proved that the spacio-temporal scale for DPD can be precisely defined by introducing the volume of a fluid particle as a new variable. The model is interesting from theoretical point of view but it is very hard for implementing efficiently in simulating multicomponent fluids. Moreover, it is less efficient involving larger cut off radius than FPM and DPD. This price paid for being more strict with matching spatio-temporal scale may appear currently too demanding especially for 3-D simulations. There is a thin border between the applicability of a numerical model and theory.

With the FPM we can extend further the capabilities of the discrete particle method to the mesoscopic regime and show that they are competitive to standard simulation techniques with continuum equations. These methods establish a foundation for cross-scale computations ranging from nanoscales to microns and can provide a framework to study the interaction of microstructures and large-scale flow, which may be of value in blood flow and other applications in polymeric dynamics.

Acknowledgements

We thank Dr Dan Kroll (MSI) for useful discussions. Support for this work was provided by the Energy Research Laboratory Technology Research Program of the Office of Energy Research of the U.S. Department of Energy under subcontract from the Pacific Northwest National Laboratory and partly by the Polish Committee for Scientific Research (KBN) Grant No. 8T11C00615.

References

[1] Moseler M and Landman U 2000 *Science* **289** 1165
[2] Ottino J M, De Roussel P, Hansen S and Khakhar D V 2000 *Advances in Chemical Engineering* **25** 105
[3] Prausnitz J and Wu J 2000 *En Vision* **16** 18
[4] Gast A P and Russel W B 1998 *Physics Today* 24
[5] Latinopoulos P and Ganoulis J 1982 *Applied Mathematical Modelling* **6** 55
[6] Misra J C and Sahu B K 1998 *Computers & Mathematics with Applications* 16/12 993
[7] Burda P and Korenar J 1996 *Akademie Verlag. Zeitschrift fur Angewandte Mathematik und Mechanik* **76** 365
[8] Gueraoui K, Hammoumi A and Zeggwagh G 1998 *Computes Rendus de l Academie des Sciences Serie II Fascicule B-Mecanique Physique Chimie Astronomie* **326** 561
[9] Groisman A and Stainberg V 2000 *Nature* **405** 53
[10] Fung Y C and Zweifach B W 1971 *Annual Review of Fluid Mechanics* **III** 189
[11] Alda W, Dzwinel W, Kitowski J, Moscinski J, Pogoda M and Yuen D A 1998 *Computers in Physics* **12** (6) 595
[12] Dzwinel W, Alda W, Pogoda M and Yuen D A 2000 *Physica* **D 137** 157
[13] Vashishta P and Nakano A 1999 *Computing in Science and Engineering* 20
[14] Wagner A J and Yeomans J M 2000 *Phys. Rev.* **E** (submitted)
[15] Chopard B and Droz M 1998 *Cellular Automata Modelling of Physical Systems* Cambridge University Press
[16] Swift M R, Orlandini E and Osbors W R 1996 *Phys. Rev.* **E 54** 5041
[17] Meakin P 1998 *Fractals, scaling and growth far from equilibrium* Cambridge University Press
[18] Choi H G and Joseph D D 2000 *University of Minnesota Supercomputing Institute Research Report* UMSI 2000/17
[19] Glowinski R, Pan T W, Hela T I, Joseph D D and Priaux J 2000 *University of Minnesota Supercomputing Institute Research Report* UMSI 2000/68
[20] Ihle T and Kroll D M 2001 *Rhys. Rev.* **E 63** 020201
[21] Talu I, Tardos G I and Khan M I 2000 *Powder Technol.* **110** 59
[22] Hoogerbrugge P J and Koelman J M V A 1992 *Europhysics Letters* **19** 3 155
[23] Español P 1998 *Phys. Rev.* **E 57** 2930
[24] Marsh C, Backx G and Ernst M H 1977 *Phys. Rev.* **E 56** 1976
[25] Coveney P V and Novik K E 1996 *Phys. Rev.* **E 54** 5134
[26] Dzwinel W and Yuen D A 2000 *International Journal of Modern Physics* **C 11** 1
[27] Dzwinel W and Yuen D A 2000 *J. Colloid Interface Science* **225** 179
[28] Dzwinel W and Yuen D A 2000 *International Journal of Modern Physics* **C 11** 1037
[29] Dzwinel W and Yuen D A 1999 *Molecular Simulation* **22** 369
[30] Clark A T, Lal M, Ruddock J N and Warren P B 2000 *Langmuir* **16** 6342
[31] Dzwinel W and Yuen D A 2001 *International Journal of Modern Physics* **C** accepted for publication
[32] Boryczko K, Dzwinel W and Yuen D A 2000 *Minnesota Supercomputing Institute Research Reports* UMSI 2000/142 and *Proceedings of 1st SGI Users Conference* Cracow, Poland ACC Cyfronet UMM 231
[33] Libersky L D, Petschek A G, Carney T C, Hipp J R and Allahdadi F A 1993 *J. Comp. Phys* **109** 67
[34] Daniel J C and Audebert R 1999 Small Volumes and Large Surfaces: The World of Colloids, in: *Soft Matter Physics* Eds. Daoud M, and Williams C E, Springer Verlag 320

[35] Grier D G and Behrens S H 2001 Interactions in colloidal suspensions in *Electrostatic effects in Soft Matter and Biphysics* Ed. Holm C, Keikchoff P, Podgornik R, Kluwer
[36] Yaman K, Jeppesen C and Marques C M 1998 *Europhys. Lett* **42** 221
[37] Larsen A and Grier D G 1997 *Nature* **385** 230
[38] Serrano M and Español P 2000 *Phys. Rev.* **E** (submitted)
[39] Hockney R W and Eastwood J W 1981 *Computer Simulation Using Particles* McGraw-Hill Inc.
[40] Kubo R 1965 *Statistical Mechanics* Wiley, New York
[41] Chapman S and Cowling T G 1990 *The Mathematical Theory of Non-uniform Gases* Cambridge University Press
[42] Español P and Serrano M 1999 *Phys. Rev.* **E 59** 6340
[43] Li Jinghai 2000 *Powder Techol.* **111** 50